

Proceedings Article

MPI reconstruction using Bessel functions

M. Maass^{1,*} · C. Droigk¹ · A. Mertins¹

¹Institute for Signal Processing, University of Lübeck, Lübeck, Germany

*Corresponding author, email: marco.maass@uni-luebeck.de

© 2020 Maass *et al.*; licensee Infinite Science Publishing GmbH

This is an Open Access article distributed under the terms of the Creative Commons Attribution License (<http://creativecommons.org/licenses/by/4.0>), which permits unrestricted use, distribution, and reproduction in any medium, provided the original work is properly cited.

Abstract

This publication proposes for the first time a direct reconstruction technique based on weighted Bessel functions of first kind. As basis for the formulation the well-known Chebyshev reconstruction is used. By utilizing the Fourier transform of Chebyshev polynomials of second kind, which is nothing else than a weighted Bessel function of first kind, a new formulation which allows for reconstruction of the particle distribution in the Fourier domain is derived. This method comes with the benefit of allowing for a direct deconvolution in frequency domain. With numerical simulations we show the equivalence to the Chebyshev reconstruction and demonstrate different strategies to perform the deconvolution.

I Introduction

In a fairly simplified model, Magnetic Particle Imaging (MPI) can be described by the Langevin theory of paramagnetism [1]. Unfortunately, the model neglects relaxation effects of the nanoparticles and magnetic field inhomogeneities of the scanner. This problem results in a lack of closed-form solutions in MPI, which made it popular to use system matrix based reconstructions when higher-dimensional drive field excitation is considered. However, if only one-dimensional excitation for the drive field is used, the model is good enough for fast image reconstruction techniques. Such common techniques are the x-space reconstruction [2] or the Chebyshev based reconstruction [3]. It was shown that, from the mathematical point of view, the Chebyshev and x-space reconstructions are completely equivalent [4]. Nevertheless, from a practical point of view both methods have their own pros and cons. A relationship between MPI and Bessel functions of first kind was uncovered in [5]. Throughout this publication we will transfer the Chebyshev based reconstruction into the spatial Fourier domain, which finally results in a Bessel series based reconstruction technique for MPI.

II 1D MPI with the Langevin model

One-dimensional MPI can be described by the model [1]

$$u(t) = \frac{d}{dt} \left[\int_{-\infty}^{\infty} c(x) M_0 \mathcal{L}(\beta G(x_{\text{FFP}}(t) - x)) dx \right] \quad (1)$$

with $\beta = \frac{\mu_0 m}{k_B T}$ and $M_0 = p \mu_0$, where $u(t)$ denotes the voltage signal, $c(x)$ is the spatial particle distribution, p denotes the coil sensitivity, μ_0 the vacuum permeability, k_B the Boltzmann's constant, T the temperature of the particles, and m the magnetic moment of one particle. The function $\mathcal{L}(x)$ denotes the Langevin function, which is used to describe the mean magnetization of the particle distribution. The position of the field-free point (FFP) at time point t is given by $x_{\text{FFP}}(t) = -G^{-1} H^D(t)$, where $H^D(t)$ denotes the drive field and G denotes the applied gradient strength of the static gradient field. One common choice for the drive field is $H^D(t) = -A \cos(2\pi f_D t)$, which is periodic with $T_D = 1/f_D$ and A denotes the drive field amplitude. Commonly, (1) is also given in terms of

Fourier series coefficients of $u(t)$:

$$u_k = \frac{1}{T_D} \int_{-T_D/2}^{T_D/2} u(t) e^{-i\omega_k t} dt, \quad (2)$$

where $\omega_k = 2\pi f_D k$. It was shown that the Chebyshev series expansion [3]

$$\tilde{c}(x) = \frac{T_D |G|}{i M_0 \pi |A|} \sum_{k=1}^{\infty} U_{k-1} \left(\frac{G}{A} x \right) u_k \quad \text{if } \left| \frac{G}{A} x \right| \leq 1 \quad (3)$$

with $U_k(x)$ being the Chebyshev polynomial of second kind and order k can be used to reconstruct the “blurred” particle distribution $\tilde{c}(x) = (c * \tilde{m})(x)$, where $*$ denotes convolution of the particle distribution $c(x)$ with $\tilde{m}(x) = m\beta G \mathcal{L}'(\beta G x)$. If desired, the function $\tilde{c}(x)$ can be deconvolved in the spatial Fourier domain with help of the Fourier transform of $\tilde{m}(x)$.

III Bessel function based reconstruction

Let

$$V_k(x) = \begin{cases} U_{k-1}(x) \sqrt{1-x^2} & \text{if } |x| \leq 1 \\ 0 & \text{else} \end{cases} \quad (4)$$

The Fourier transform of $V_k(x)$ with $k \in \mathbb{N}_+$ reads

$$\hat{V}_k(\alpha\omega) = \mathcal{F} \left\{ \frac{1}{a} V_k \left(\frac{x}{a} \right) \right\} = \frac{-k\pi J_k(\alpha\omega)}{i^{k+1} \alpha\omega}, \quad (5)$$

where $J_k(\omega)$ denotes the Bessel function of first kind and order k . The “blurred” concentration $\tilde{c}(x)$ according to (3) is now weighted to yield

$$\begin{aligned} q(x) &= \sqrt{1 - \left(\frac{G}{A} x \right)^2} \tilde{c}(x) = V_1 \left(\frac{G}{A} x \right) \tilde{c}(x) \\ &= \frac{T_D |G|}{i M_0 \pi |A|} \sum_{k=1}^{\infty} V_k \left(\frac{G}{A} x \right) u_k. \end{aligned} \quad (6)$$

By applying the spatial Fourier transform to each term in (6), one obtains

$$\hat{q}(\omega) = \frac{T_D G}{M_0 A} \sum_{k=1}^{\infty} \frac{k J_k \left(\frac{A}{G} \omega \right)}{i^k \omega} u_k. \quad (7)$$

The final deconvolution problem now reads

$$\hat{q}(\omega) = \frac{1}{2\pi} \frac{|A|}{|G|} \hat{V}_1 \left(\frac{A}{G} \omega \right) * (\tilde{c}(\omega) \cdot \hat{m}(\omega)). \quad (8)$$

Although multiplication and convolution do not exactly commute, a strategy to obtain the deconvolved particle distribution from $\hat{q}(\omega)$ could be to multiply (8) with the reciprocal of $\hat{m}(\omega)$, then perform an inverse fast Fourier transform (IFFT), and finally weight the result with the inverse of $V_1(x)$ to obtain an estimate of $c(x)$. Alternatively,

it can be observed that the “blurred” particle distribution has the form

$$\tilde{c}(x) = \frac{1}{\sqrt{1 - \left(\frac{G}{A} x \right)^2}} q(x) \quad (9)$$

and, equivalently, the formula (9) reads in frequency space

$$\hat{\tilde{c}}(\omega) = \frac{|A|}{2|G|} J_0 \left(\frac{A}{G} \omega \right) * \hat{q}(\omega). \quad (10)$$

Eq. (10) allows one to perform a numerical deconvolution with $J_0 \left(\frac{A}{G} \omega \right)$. To carry out the deconvolution, an additional windowing function has to be applied, otherwise the deconvolution with the Bessel function of first kind and order zero becomes unstable. Afterward, $\hat{\tilde{c}}(\omega)$ has to be multiplied with the reciprocal of $\hat{m}(\omega)$ to obtain the Fourier transformed particle distribution $\hat{c}(\omega)$.

IV Material and methods

Based on the Langevin model of paramagnetism, simulations of a one dimensional MPI system were carried out to obtain a voltage signal $u(t)$. Afterward, the voltage signal was corrupted with white Gaussian noise so that the signal-to-noise ratio was 15 dB. Next, the FFT was used to compute the frequency components u_k . The particle size was set to 30 nm and human body temperature was assumed. The applied gradient field strength was $G = 1 \text{ T}/((m\mu_0))$ and the drive field amplitude was $A = 0.0125 \text{ T}/\mu_0$. This resulted in a field of view of 23 mm. Moreover, we set f_D to 26.04 kHz. The deconvolution was performed by an pseudoinverse filtering with $\hat{m}^{-1}(\omega)$ and the cutoff frequency ω_c when $|\hat{m}^{-1}(\omega_c)| = 0.1 |\hat{m}^{-1}(0)|$.

V Results and discussion

Fig. 1 shows different reconstruction results for a ground truth phantom. In the top row, the reconstruction results were obtained without deconvolution $\tilde{c}(x)$, whereas at the bottom, the reconstructions were performed with deconvolution of $\tilde{c}(x)$. The plot titles describe the steps taken to obtain the reconstructions. In the left column, the baseline Chebyshev reconstruction is shown. The middle and right columns show the image reconstructions using the proposed strategies based on Eq. (7). In the middle, the weighting $V_1(G/Ax)$ was removed in the image domain (ID) (9). The middle plot at the bottom shows the result for a deconvolution in frequency domain (FD) with $\hat{m}^{-1}(\omega)$ (8) followed by removing the weighting in ID (9). Although this procedure is mathematically not entirely correct to yield the true particle distribution, the reconstruction is quite similar to the other ones. Only near to the FOV boundaries, some singularities become visible. Overall, this strategy is the

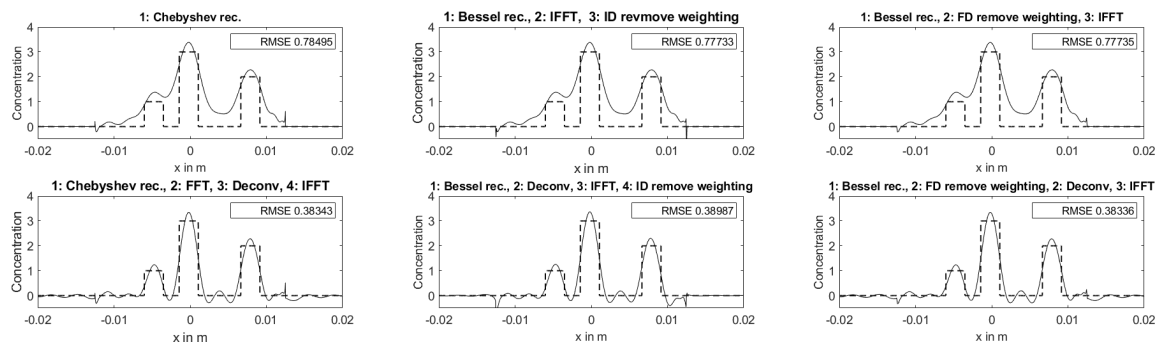


Figure 1: Results of different reconstruction methods. Top: Reconstructions of $\tilde{c}(x)$. Bottom: Reconstructions of $c(x)$ with deconvolution of $\tilde{c}(x)$ (Deconv). The ground truth distribution is indicated by dashes. The titles describe the operations carried out to obtain the reconstructions. The shorthand FD stand for an operation in frequency domain and ID means an operation in image domain. FFT and IFFT denote the fast Fourier transform and its inverse, respectively. RMSE denotes the root mean squared error related ground truth distribution.

most efficient one of the shown methods with deconvolution of $\tilde{c}(x)$. The right plots show the reconstruction results after removing the weighting in the FD (10). The top right plot is equivalent to the result after applying Eq. (10) followed by an IFFT. At the right bottom, also a deconvolution with $\hat{m}^{-1}(\omega)$ (8) was performed, and it can be observed that the reconstruction is nearly identical to the Chebyshev based reconstruction with deconvolution shown on the left side.

VI Conclusions

We proposed a direct image reconstruction for one-dimensional MPI which is fully equivalent to the Chebyshev reconstruction. The proposed method allows for reconstruction of the particle distribution in the frequency domain. Since deconvolution is commonly performed in the frequency domain, the proposed method is well suited for such purpose. Interestingly, inserting (7) into (10) uncovers a convolution structure between different Bessel functions of first kind, which should be further investigated.

Author's Statement

The author state no funding involved. Authors state no conflict of interest.

References

- [1] T. Knopp and T. M. Buzug. Magnetic Particle Imaging: Introduction to Imaging Principles and Scanner Instrumentation. Springer Berlin/Heidelberg, 2012.
- [2] P. W. Goodwill and S. M. Conolly. Multidimensional X-Space Magnetic Particle Imaging. *IEEE Trans. Med. Imag.*, vol. 30-9, pp. 1581–1590, 2011.
- [3] J. Rahmer, J. Weizenecker, B. Gleich, and J. Borgert. Signal encoding in magnetic particle imaging: properties of the system function. *BMC Medical Imaging*, vol. 9-4, 2009.
- [4] M. Grüttner, T. Knopp, J. Franke, M. Heidenreich, J. Rahmer, A. Halkola, C. Kaethner, J. Borgert, and T. M. Buzug. On the formulation of the image reconstruction problem in magnetic particle imaging. *Biomed. Tech.*, vol 58-6, pp. 583–591, 2012.
- [5] M. Maass, and A. Mertins. On the Formulation of the Magnetic Particle Imaging System Function in Fourier Space. *Int. Workshop Magn. Part. Imaging*, pp. 39-40, 2018.